Longitudinal mode multistability in Ring and Fabry-Pérot lasers: the effect of spatial hole burning

A. Pérez-Serrano,[1,*] **J. Javaloyes,**[2] **and S. Balle**[3]

[1]*IFISC (UIB-CSIC), C/ Valldemossa km. 7'5, E-07122 Palma de Mallorca, Spain*
[2]*Dept. of Electronics and Electrical Engineering, University of Glasgow, UK*
[3]*IMEDEA (UIB-CSIC), C/ Miquel Marqués 21, E-07190 Esporles, Spain*

**antonio@ifisc.uib-csic.es*

Abstract: We theoretically discuss the impact of the cavity configuration on the possible longitudinal mode multistability in homogeneously broadened lasers. Our analysis is based on the most general form of a Travelling-Wave Model for which we present a method that allows us to evaluate the monochromatic solutions as well as their eigenvalue spectrum. We find, in agreement with recent experimental reports, that multistability is more easily reached in Ring than in Fabry-Pérot cavities which we attribute to the different amount of Spatial-Hole Burning in each configuration.

OCIS codes: (140.3430) Laser theory; (140.3410) Laser resonators; (140.3560) Lasers, ring.

References and links

1. C. J. Born, S. Yu, M. Sorel, and P. J. R. Laybourn, "Controllable and stable mode selection in a semiconductor ring laser by injection locking," in *CLEO Proceedings*, paper CWK4, (2003).
2. C. J. Born, M. Hill, S. Yu, and M. Sorel, "Study of longitudinal mode coupling in a semiconductor ring laser," in *Proceedings of the 17th Annual Meeting of the IEEE-LEOS*, pp. 27–28 (2004).
3. C. J. Born, M. Sorel, and S. Yu, "Linear and nonlinear mode interactions in a semiconductor ring laser," IEEE J. Quantum Electron. **41**, 261 (2005).
4. Z. Wang, G. Yuan, G. Verschaffelt, J. Danckaert, and S. Yu, "A novel semiconductor ring laser device aimed for all-optical signal processing," in *ECOC Proceedings*, paper Th.1.C.4 (2008).
5. M. Sorel, P. J. R. Laybourn, G. Giuliani, and S. Donati, "Unidirectional bistability in semiconductor waveguides lasers," Appl. Phys. Lett. **80**(17), 3051–3053 (2002).
6. K. Huybrechts, B. Maes, G. Morthier, and R. Baets, "Tristable all-optical flip-flop using coupled non linear cavities," in *Winter Topical Meeting Series* (IEEE, New York, 2008), p. 1617.
7. L. M. Narducci, J. R. Tredicce, L. A. Lugiato, N. B. Abraham, and D. K. Bandy, "Mode-mode competition and unstable behavior in a homogeneously broadened ring laser," Phys. Rev. A **33**, 1842 (1986).
8. L. A. Kotomtseva, "Steady states for longitudinal modes and dynamics of a laser with a saturable absorbent," Quantum Semiclass. Opt. **10**, 331 (1998).
9. R. Lang and K. Kobayashi, "External optical feedback effects on semiconductor injection-laser properties," IEEE J. Quantum Electron. **16**, 347 (1980).
10. A. Loose, B. K. Goswami, H.-J. Wünsche, and F. Henneberger, "Tristability of a semiconductor laser due to time-delayed optical feedback," Phys. Rev. E **79**, 036211 (2009).
11. K. P. Komarov, "Multistable single-mode emission from solid-state state lasers," Quantum Electron. **24**(11), 975–976 (1994).
12. J. R. Tredicce, L. M. Narducci, N. B. Abraham, D. K. Bandy, and L. A. Lugiato, "Experimental-evidence of mode competition leading to optical bistability in homogenously broadened lasers," Opt. Commun. **56**, 435 (1986).
13. M. Yamada, "Theory of mode competition noise in semiconductor injection-lasers," IEEE J. Quantum Electron. **22**, 1052 (1986).
14. F. Pedaci, S. Lepri, S. Balle, G. Giacomelli, M. Giudici, and J. R. Tredicce, "Multiplicative noise in the longitudinal mode dynamics of a bulk semiconductor laser," Phys. Rev. E **73**, 041101 (2006).

#136640 - $15.00 USD Received 18 Oct 2010; revised 20 Dec 2010; accepted 23 Dec 2010; published 4 Feb 2011

15. T. Acsente, "Laser diode intensity noise induced by mode hopping," Romanian Rep. Phys. **59**, 87 (2007).
16. Ya. I. Khanin, *Fundamentals of Laser Dynamics*, Cambridge Int. Sci. Pub. Ltd., Cambridge, UK (2006).
17. H. Fu and H. Haken, "Multifrequency operations in a short-cavity standing-wave laser," Phys. Rev. A **43**, 2446–2454 (1991)
18. L. A. Lugiato, L. M. Narducci, and M. F. Squicciarini, "Exact linear-stability analysis of the plane-wave Maxwell-Bloch equations for a ring laser," Phys. Rev. A **34**, 3101 (1986).
19. G. J. de Valcárcel, E. Roldán, and F. Prati, "Risken-Nummedal-Graham-Haken instability in class B lasers," Opt. Commun. **163**, 5–8 (1999).
20. H. Risken and K. Nummedal, "Self-pulsing in lasers," J. Appl. Phys. **39**, 4662 (1968).
21. R. Graham and H. Haken, "Quantum theory of light propagation in a fluctuating laser-active medium," Z. Phys. **213**, 420 (1968).
22. A. Pérez-Serrano, J. Javaloyes, and S. Balle, "Bichromatic emission and multimode dynamics in bidirectional Ring Lasers," Phys. Rev. A **81**, 043817 (2010).
23. J. Javaloyes and S. Balle, "Quasiequilibrium time-domain susceptibility of semiconductor quantum wells," Phys. Rev. A **81**, 062505 (2010).
24. S. Fürst, A. Pérez-Serrano, A. Scirè, M. Sorel, and S. Balle, "Modal structure, directional and wavelength jumps of integrated semiconductor ring lasers: Experiments and theory," Appl. Phys. Lett. **93**, 251109 (2008).
25. R. J. LeVeque, *Finite Difference Methods for Ordinary and Partial Differential Equations, Steady State and Time Dependent Problems*, Society for Industrial and Applied Mathematics (SIAM), Philadelphia, (2007).
26. J. W. Eaton, *GNU Octave Manual*, Network Theory Limited, (2002).

Several recent reports [1–4] experimentally demonstrate that the emission wavelength of bidirectional semiconductor ring lasers (SRL) can be selected by optical injection among that of several longitudinal modes; upon removal of the optical injection, the emission wavelength remains stable at the chosen value. In addition, wavelength multistability in SRLs can coexist with the directional bistability [5], hence it can be of interest for all-optical signal processing applications at a higher-logical level [6]. Although early studies of unidirectional ring lasers, where only one propagation direction was allowed, suggested possible multistability among longitudinal modes [7, 8], this behavior has, to our knowledge, never before been explained or experimentally observed in other types of single-cavity free-running devices lasers.

Multistable behavior has been observed in more complex configurations as lasers with optical feedback [9, 10] or with intracavity saturable absorbers [11]. Notice also that it was shown that a carefully chosen detuning can induce a degeneracy between two adjacent modes and promote bistability in Fabry-Pérot (FP) CO_2 laser [12]. Also, in FP semiconductor lasers, one should mention stochastic mode-hopping between two adjacent modes that consists of random jumps with short characteristic times (below 1 ms) from one stable mode to the other induced by spontaneous emission noise [13, 14] or, in general, by parameter fluctuations [15] that change the tuning of the gain with respect to the cavity. Yet, at variance with SRL, in these cases there is no evidence that the emission wavelength can be selected at will and remain for long periods.

The different behavior of SRL and FP lasers regarding wavelength multistability calls for an explanation. However, ascertaining multistability requires the determination of the monochromatic solutions and the resolution of the linear stability analysis (LSA). These two problems are known to be difficult if not impossible to implement analytically in the general case, and solutions are only available under strong approximations. Within the Uniform Field Limit (UFL) approximation [7], this can be accomplished via a modal decomposition for either ring [16] or FP lasers [17]. Beyond the UFL, analytical results are available for unidirectional rings if one neglects internal losses [18] and/or invokes singular perturbation techniques [19]. When bidirectional emission, cavity losses or spatially dependent parameters come into play, no general method for the LSA is known, which hinders the study of many devices as bidirectional SRL, FP lasers, or devices for which the UFL or singular perturbations methods are inadequate.

In this paper we compare bidirectional ring and FP lasers regarding the possible multistability of their longitudinal modes. We present numerical methods –independent of the boundary conditions and of parameter values – that allow for determining any monochromatic solution

#136640 - $15.00 USD Received 18 Oct 2010; revised 20 Dec 2010; accepted 23 Dec 2010; published 4 Feb 2011

by a low dimensional shooting procedure. The LSA is obtained by constructing the linearized evolution operator for which we can evaluate the Floquet multipliers and trace back the eigenvalues governing the stability. Our approach is quite general and could also be applied to other dynamical systems described by partial differential equations (PDE)s, and our results extend and generalize the previous studies performed for unidirectional ring lasers [7, 18–21]. We find that multistability is more easily reached in rings as compared to FP cavities, because of the different amounts of Spatial-Hole Burning in each configuration.

We consider homogeneously broadened lasers described by the bidirectional Travelling-Wave Model (TWM) (see [22] and references therein) that reads

$$
\begin{aligned}
(\pm\partial_s + \partial_\tau)A_\pm &= B_\pm - \alpha A_\pm \ , && (1)\\
\gamma^{-1}\partial_\tau B_\pm &= -(1+i\delta)B_\pm + g(D_0 A_\pm + D_{\pm 2}A_\mp) \ , && (2)\\
\varepsilon^{-1}\partial_\tau D_0 &= J - D_0 - (A_+ B_+^* + A_- B_-^* + c.c.) \ , && (3)\\
\eta^{-1}\partial_\tau D_{\pm 2} &= -D_{\pm 2} - \varepsilon\eta^{-1}(A_\pm B_\mp^* + A_\mp^* B_\pm) \ , && (4)
\end{aligned}
$$

where $A_\pm$ are the scaled slowly varying amplitudes of the counter-propagating electric fields, $B_\pm$ are their respective polarizations, D_0 is the quasi-homogeneous inversion density and $D_{\pm 2}$ are the spatially-dependent contributions to the grating in the population inversion density that arise from standing wave effects and lead to saturation of the gain. Space and time (s,τ) are scaled by the length L_c and the time of flight τ_c of the cavity, respectively. α are the internal losses per unit length, γ determines the spectral width of the gain spectrum, δ is the detuning, and ε and η are the decay times for D_0 and $D_{\pm 2}$ respectively, which differ due to the impact of diffusion on the decay of the grating terms. Although this model does not correctly describe

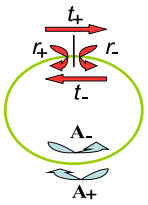

$$
\begin{aligned}
A_+(0,\tau) &= t_+ A_+(1,\tau) + r_- A_-(0,\tau)\\
A_-(1,\tau) &= t_- A_-(0,\tau) + r_+ A_+(1,\tau)
\end{aligned}
$$

Fig. 1. General cavity structure and boundary conditions.

the asymmetric gain curve typical of semiconductor materials as it lacks the strong amplitude-phase coupling denoted by Henry's linewidth enhancement factor α_H, it still can shed some light on the different behavior of ring and FP lasers regarding multistability. One can expect α_H to induce an asymmetry of the multistability band around the dominant mode, but a precise analysis of semiconductor devices requires modelling the material response as in e.g. [23]. Since in the TWM the field evolution is governed by a PDE, it is possible to treat on equal grounds ring and FP cavities simply by supplying for the appropriate boundary conditions. For the sake of simplicity we consider that the atomic line is resonant with a cavity mode (i. e., $\delta = 0$), hence the boundary conditions are written in Fig. 1, where $r_\pm$ and $t_\pm$ denote the reflectivity and transmissivity of the forward and backward waves.

The TWM admits multiple monochromatic solutions that might be stable above their lasing threshold, given by their branching points on the off state $D_0 = J, A_\pm = B_\pm = D_{\pm 2} = 0$ [22, 24]. For instance, for a pure ring cavity ($r_\pm = 0$), the frequency ($\omega_m^\pm$) and threshold ($J_m^\pm$) for mode m in each of the counter-propagating directions read

$$
\omega_m^\pm = \frac{2\pi m}{1+\alpha_{tot}^\pm/\gamma} \ , \quad J_m^\pm = \frac{\alpha_{tot}^\pm}{g}\left[1+\left(\frac{\omega_m^\pm}{\gamma}\right)^2\right] \ , \qquad (5)
$$

#136640 - $15.00 USD Received 18 Oct 2010; revised 20 Dec 2010; accepted 23 Dec 2010; published 4 Feb 2011

where $\alpha_{tot}^{\pm} = \alpha - \ln t_{\pm}$ denotes the total distributed loss in each propagation direction. In the same way for a FP cavity ($t_{\pm} = 0$), we have —with $\alpha_{tot} = \alpha - \ln\sqrt{r_+ r_-}$—

$$\omega_m = \frac{\pi m}{1 + \alpha_{tot}/\gamma}\,, \quad J_m = \frac{\alpha_{tot}}{g}\left[1 + \left(\frac{\omega_m}{\gamma}\right)^2\right]\,. \tag{6}$$

Assessing modal multistability requires finding the monochromatic solutions of Eqs. (1)-(4) and determining their stability for a given operation point. We compute the modes for a given cavity configuration via a shooting method. With an initial guess for the modal frequency and amplitudes $A_{\pm}(0)$, we solve for the spatial dependence of (1)-(4) using standard integration techniques with a spatial step $h = 1/N$ towards the other end of the cavity, where the propagated values $A_{\pm}(1)$ must verify the boundary conditions. By using a Newton-Raphson algorithm a new guess for the field amplitudes $A_{\pm}(0)$ and the modal frequency is proposed and the process is repeated until one reaches convergence. The final trajectory generated by this shooting method provides a discretized representation of the modal profile as a spatial mesh of N points.

From the monochromatic solutions, one could in principle compute the eigenvalues from the linearized form of Eqs. (1)–(4). However, the resulting system is still a hyperbolic PDE, and a discrete representation of the solution would require to express the gradient operator using finite differences. This approach is not practical: time propagation of hyperbolic PDEs cannot be made reliably for an arbitrary choice of the spatial and of the temporal discretization, leading to large errors in the eigenvalues. Instead, we use the temporal map $\mathbf{V}_{n+1} = \mathbf{U}(h, \mathbf{V}_n)$ described in [22] that advances the state vector $\mathbf{V}$ a time step h while verifying the Courant condition [25] and cancelling numerical dissipation. We then consider all possible perturbations of $\mathbf{V}$ hereby finding the matrix $\mathbf{M} = \partial\mathbf{U}/\partial\mathbf{V}$ representing the linear operator governing the time evolution for the perturbations around one given monochromatic solution. We finally compute the $11 \times N$ Floquet multipliers z_i of $\mathbf{M}$, which determine the eigenvalues as $\lambda_i = h^{-1}\ln z_i$. We used $N = 256$ mesh points; in this case, determining the spatial profile of the monochromatic solution, generating the matrix $\mathbf{M}$ and diagonalizing it using the QR decomposition method takes 1, 10 and 60 seconds, respectively, on an standard PC using C++ routine based on *Octave* [26]. Stability results have been controled by direct integration of the TWM [22]. In the following pictures, solid (dashed) lines represent the stable (unstable) solutions and parameters are typical of III-V semiconductor systems: a cavity of $L_c = 2.4$ mm and $\tau_c = 25$ ps, a modal gain of 33 cm^{-1}, a gain width of 13 nm, a carrier lifetime 0.5 ns and a diffusion coefficient of 5 cm^2/s.

The results are shown in Fig. 2 for the solution $m = 2$ of a symmetric, bidirectional ring laser. In panel a) we show that just above the threshold current $J \simeq 0.51$, this solution corresponds to an unstable bidirectional state. At $J_{\in} \simeq 1.5$, a pitchfork bifurcation into unidirectional emission occurs, but the degenerate (almost) unidirectional states are also unstable, as evidenced by the eigenvalues shown in panel b) for $J = 3$. However, for currents above $J > 3.5$, they become stable and all the eigenvalues have $Re(\lambda) < 0$ (see panel c) for $J = 4$).

Repeating this procedure for all solutions allows us to obtain a general view of the stability of the system by plotting the bifurcation diagrams for all modes. In our case, however, it suffices to examine only half of the diagram because the resonance condition implies symmetry for $\pm m$.

Figure 3 depicts the general bifurcation diagram for both the ring laser with the parameters in Fig. 2 (panel a), and an equivalent FP device (panel b). In this sense, a word of caution is in order: for a fair comparison of the behavior of the two devices, both should work with the same degree of gain saturation, hence the pump density and the threshold pump density should be the same in both cases. Since the lasing condition in ring lasers involves a single pass in the cavity, while that of FP lasers implies a roundtrip, the length of the FP cavity should be one half of that of the ring provided that the total distributed losses are the same in both cases. In this way, moreover, the frequency spacing of the modes and their threshold gain difference are

#136640 - $15.00 USD Received 18 Oct 2010; revised 20 Dec 2010; accepted 23 Dec 2010; published 4 Feb 2011

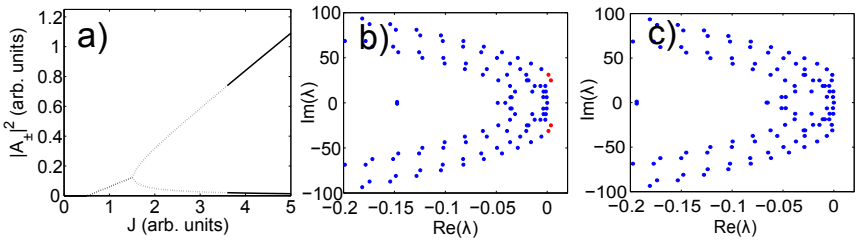

Fig. 2. (a) Numerical bifurcation diagram for mode $m = 2$ for a ring laser, $g = 4$, $\gamma = 250$, $\alpha = 2.03$, $\varepsilon = 0.05$, $\eta = 10$, $t_+ = t_- = 0.98$ and $r_+ = r_- = 0.01$. The threshold value is $J_{th} = 0.51$. (b) Real versus imaginary part of the eigenvalues for $J = 3$. Eigenvalues in blue (red) have $Re(\lambda) < 0$ ($Re(\lambda) > 0$). (c) Same as panel (b) for $J = 4$.

the same in both configurations. Thus, the scaled parameters g, γ, ε, and η of a ring laser have to be twice their equivalent FP values. For the parameters of Fig. 2, the ring laser just above threshold has only one stable solution $m = 0$. Upon increasing J, this bidirectional solution becomes unstable first via a Hopf bifurcation at $J \sim 0.7$ and then via a pitchfork bifurcation at $J_\in \sim 1.5$ that leads to two symmetrical, almost unidirectional, solutions. Although the solutions corresponding to $m = 3$ remain unstable over the interval of J shown, solutions $m = 1$ and $m = 2$ become stable for high enough J, hence the system easily displays multistability once in the almost unidirectional regime. The equivalent FP laser behaves remarkably different from the ring laser regarding multistability (see Fig. 3b). Above threshold, the mode $m = 0$ starts lasing stably, but when the pump is increased it quickly becomes unstable through a multimode instability [17]. All the other modes are unstable over all the pump interval examined.

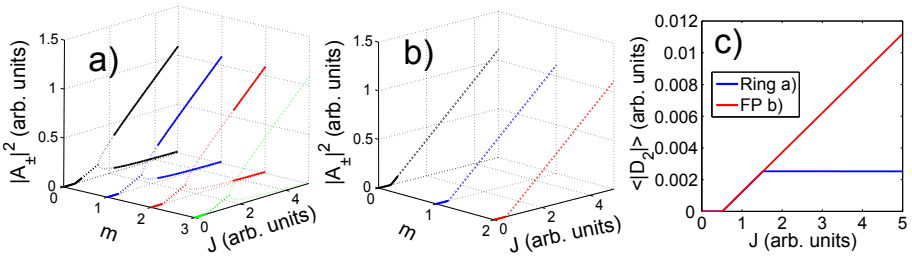

Fig. 3. Bifurcation diagram for the first modes of a ring laser (a) with the parameters of Fig. 2 and for an equivalent FP laser (b), $g = 2$, $\gamma = 125$, $\alpha = 1.01$, $\varepsilon = 0.025$, $\eta = 5$, $t_\pm = 0$ and $r_\pm = 0.99$. (c) $< |D_2| >$ is the average of $|D_2|$ along the cavity for cases (a) and (b).

The results in Fig. 3 correspond to the UFL, but our methodology allows us to easily address their robustness regarding the cavity losses. We can confirm that, in this case, non uniform field amplitudes do not qualitatively modify the multistability scenario as shown in Fig. 4, where we plot the results obtained for a high-loss ring laser (panel a) and two equivalent FP lasers, one symmetric (panel b) and one highly asymmetric (panel c). Again, while the ring laser shows multistability, we never observe multistability for the FP cavities.

The physical reason for such a different behavior of FP and ring lasers is the quite different degree of spatial hole burning in the gain, as shown in Figs. 3 (panel c) and 4 (panel d), where we plot the absolute value of D_2 averaged along the cavity at different pumping levels for mode $m = 0$ of the lasers in Figs. 3 and 4, respectively. D_2 is almost the same for all modes of a given laser due to the minute modal gain differences. In the ring laser, $|D_2|$ saturates at a

#136640 - $15.00 USD Received 18 Oct 2010; revised 20 Dec 2010; accepted 23 Dec 2010; published 4 Feb 2011

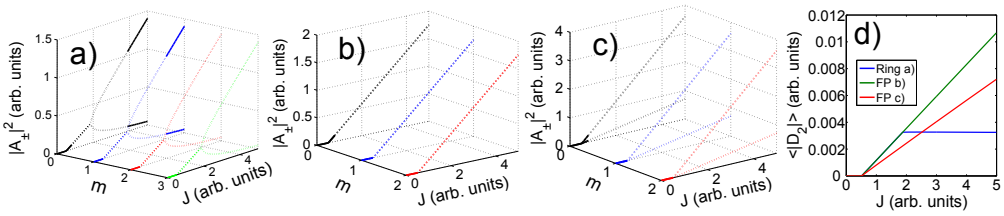

Fig. 4. Bifurcation diagram for: (a) ring laser with parameters $g = 4$, $t_{\pm} = 0.6$, $r_{\pm} = 0.01$, $\gamma = 250$, $\alpha = 1.55$, $\varepsilon = 0.05$, $\eta = 10$; (b) equivalent symmetric FP with $\alpha = 0.51$, $\eta = 5$ and $r_{\pm} = 0.6$; (c) equivalent asymmetric FP with $\alpha = 0.21$, $\eta = 5$ and $r_{+} = 0.99$ and $r_{-} = 0.2$. The threshold value is $J_{th} = 0.51$. (d) $< |D_2| >$ vs J for these lasers.

comparatively low value as soon as the pitchfork bifurcation leading to unidirectional operation occurs; for FP configurations, instead, the necessarily higher reflectivity of the facets makes $|D_2|$ larger than in the equivalent ring, and it increases continuously with the pump level.

To confirm that the grating term is what destroys multistability in the FP configuration, we consider a system with higher diffusion, which should reduce the values of D_2 (see Eq. (4)). In fact, as shown in Fig. 5, now both FP configurations display multistability among longitudinal modes because now the spatial average of D_2 (Fig. 5 panel c) is half that in Fig. 4 (panel d).

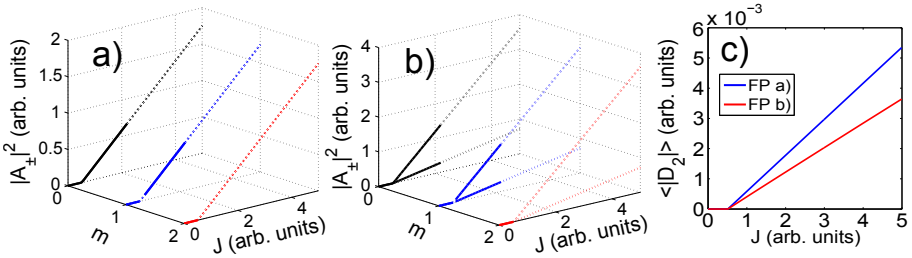

Fig. 5. Bifurcation diagram for the first three modes for a symmetric (a) and asymmetric (b) Fabry-Pérot lasers. In both cases $\eta = 10$, for other parameters see Fig. 4. (c) $< |D_2| >$ vs J for the FPs (a) and (b).

Therefore, high-quality SRL, with low reflectivity couplers, allow to observe longitudinal mode multistability much more easily than their equivalent FP configurations. Lasing in the latter requires high-enough facet reflectivities, which in turn generate substantial gain gratings that impede multistability because the self-saturation of the modal gain is larger than the cross-saturation. The former, instead, easily pass to a regime of almost unidirectional emission where the gain grating is small, and self-saturation is smaller than cross-saturation. FP devices can exhibit multistability if diffusion is strong enough to wash out the grating effectively: in this limit the grating lifetime is much shorter than carrier lifetime, and cross-saturation dominates over self-saturation.

Acknowledgements

We acknowledge support from the Govern Balear (A.P.), EPSRC (J.J., project EP-E065112-1) and project ALAS (S.B., project TEC2009-14581-C02-01).

#136640 - $15.00 USD Received 18 Oct 2010; revised 20 Dec 2010; accepted 23 Dec 2010; published 4 Feb 2011